ELSEVIER

Journal of Microbiological Methods 40 (2000) 125–134

Journal of Microbiological Methods

www.elsevier.com/locate/jmicmeth

Widefield deconvolution epifluorescence microscopy combined with fluorescence in situ hybridization reveals the spatial arrangement of bacteria in sponge tissue

Werner Manz[a,*], Gernot Arp[b], Gabriela Schumann-Kindel[a], Ulrich Szewzyk[a], Joachim Reitner[b]

[a]*Technische Universität Berlin, Institut für Technischen Umweltschutz, Fachgebiet Ökologie der Mikroorganismen, Sekretariat OE 5, Franklinstraße 29, D-10587 Berlin, Germany*

[b]*Institut und Museum für Geologie und Paläontologie, Universität Göttingen, D-37077 Göttingen, Germany*

Received 8 July 1999; received in revised form 27 July 1999; accepted 8 August 1999

Abstract

Widefield deconvolution epifluorescence microscopy (WDEM) combined with fluorescence in situ hybridization (FISH) was performed to identify and characterize single bacterial cells within sections of the mediterranean sponge *Chondrosia reniformis*. Sponges were embedded in paraffin wax or plastic prior to the preparation of thin sections, in situ hybridization and microscopy. Serial digital images generated by widefield epifluorescence microscopy were visualized using an exhaustive photon reassignment deconvolution algorithm and three-dimensional rendering software. Computer processing of series of images taken at different focal planes with the deconvolution technique provided deblurred three-dimensional images with high optical resolution on a submicron scale. Results from the deconvolution enhanced widefield microscopy were compared with conventional epifluorescent microscopical images. By the application of the deconvolution algorithm on digital image data obtained with widefield epifluorescence microscopy after FISH, the occurrence and spatial arrangement of *Desulfovibrionaceae* closely associated with micropores of *Chondrosia reniformis* could be visualized.

Keywords: Widefield deconvolution epifluorescence microscopy; FISH; 16S rRNA oligonucleotide probes; Sponge associated bacteria; *Chondrosia reniformis*

1. Introduction

Fluorescence in situ hybridization (FISH) is a modern microbiological technique for the identification and characterization of single bacterial cells in complex natural samples without prior cultivation. This technique is commonly applied to suspensions of bacteria, bacterial aggregates and biofilms (Amann et al., 1995). To detect microorganisms in situ within tissues or thick biofilms in their natural spatial distribution, embedding and sectioning of the samples prior to the hybridization procedure is necessary. For this purpose, paraffin sections have been shown to be suitable for in situ hybridizations (Poulsen et al., 1994; Licht et al., 1996; Rothemund et al., 1996). Alternatively, hard setting resins (2-

*Corresponding author. Tel.: +49-30-314-25589; fax: +49-30-314-73461.

E-mail address: manz0654@mailszrz.zrz.tu-berlin.de (W. Manz)

0167-7012/00
PII: S0167-7012(99)00103-7

hydroxyethyl-methacrylate) have been applied for embedding (Gerrits and Smid, 1983) that are suitable for hybridizations because of their relatively hydrophilic properties (Moter et al., 1998).

However, the application of in situ probing combined with conventional widefield epifluorescence microscopy is often impaired by inherent problems, e.g. thickness of the samples (tissue sections) or background fluorescence caused by out-of-focus blur, which obliterate specific signals of the fluorescent probes and may limit the applicability of the FISH technique. Thus, small objects and structures remain invisible and fluorescently labeled cells are hardly detectable within these blurred images.

One possible way to circumvent these problems is the combination of FISH with confocal laser scanning microscopy (Wagner et al., 1994; Manz et al., 1995; MacNaughton et al., 1996). Using CLSM, thickness of the specimen is not limiting since light from out-of-focus planes is physically excluded by the detector pinhole. In addition, the series of 2D digital images obtained by CLSM allows numerous digital image processings including 3D rendering and reconstructions (Lawrence et al., 1996). Limitations of CLSM are that the detector pinhole system reduces the amount of light that may enter the detector system, the strong bleaching effects caused by the laser beam used as light source and the expensive microscopical and computing equipments.

In the present approach, we demonstrate that the combination of FISH with conventional widefield epifluorescence microscopy and the subsequent application of deconvolution algorithm provides a suitable, low-cost alternative to confocal laser scanning microscopy. Deconvolution refers to the mathematical removal, or deblurring of out-of-focus haze of a certain two dimensional image obtained with an optical microscope. For that purpose, a series (stack) of digitalized optical sections from defined depths at the same *xy* location of the sample is required. A computer then compiles the information of the focus plane by reassigning signals which originated from objects located in other focal planes.

The out-of-focus blur can be mathematically modeled as a point spread function (Shaw and Rawlins, 1991) and deconvolution microscopy can therefore be thought of as a method for inverting the unavoidable and natural blurring effect of the point spread function (Holmes et al., 1995). Linear, non-iterative algorithms, such as the nearest-neighbour method, are commonly used for a quick image restoration. However, the nearest-neighbor method is considered as the least accurate and the most artificial of the algorithms available, and is therefore most often used for quick previews (Holmes et al., 1995). Deconvolution based on a measured point spread function is considered to be the more accurate image restoration compared to theoretical functions (Carrington et al., 1995) because the distortion by non-ideal optics of the microscope and filter sets is taken into account and the out-of-focus signals are placed back to the points from which they came (‘photon reassignment processing’).

Deconvolution can be combined for images acquired using transmitted light brightfield, widefield fluorescence, or confocal fluorescence microscopes. The combination of FISH with conventional epifluorescence microscopy and subsequent deconvolution rendering of series of 2D digital images may have useful implications for the in situ identification of bacteria in a wide range of specimen.

Recently, sponge-associated bacteria (SAB) were characterized by a top-to-bottom directed in situ hybridization approach using fluorescent rRNA targeted oligonucleotide probes (Schumann-Kindel et al., 1997). This study resulted in the visualization of a great amount of bacteria displaying remarkable metabolic potential, which could be assigned to the alpha-, gamma- and delta-subclass of *Proteobacteria*. However, strong blurring effects caused by out-of-focus fluorescence and low average hybridization signal intensities obstructed a more detailed elucidation of the sponge–bacteria association. In the study reported here, we demonstrate that the combination of embedding and thin-sectioning of sponge material followed by FISH and deconvolution enhanced widefield microscopy is an excellent tool to surpass these problems and provide new insights into the microbial ecology of these important invertebrates.

2. Material and methods

2.1. Sample preparation

Sample fixation was done essentially following the protocol of Manz et al. (1992). Minor modifications were needed as sponge tissue was used instead of

cell suspensions. Complete native sponges were soaked with 3.7% formalin and fixed for 4–12 h at 4–7°C. Fixed sponges were washed twice with 1× PBS (130 mM NaCl, 10 mM Na-phosphate buffer, pH 7.2) for 15 min, and stored in a 1:1 mixture (v/v) of 1× PBS and 96% (v/v) ethanol at −20°C. Tissue blocks (10×10 mm) were cut from different parts of the sponges using a sterile razor blade, dehydrated (50, 80 and 96% (v/v) ethanol, 3 min each; 2× 100% xylene, 15 min each) and subsequently embedded in paraffin. Paraffin sections of 15–20-μm thickness were obtained by using a rotary microtome HM 340 E (Microm, Walldorf, Germany) with single-use blades. The slices were mounted on silanized glass slides, dewaxed by xylene treatment for 10 min and subsequently air-dried prior to hybridization. Subsamples of the sponge material were embedded in Technovit 7100 (2-hydroxyethylmethacrylate, Heraeus Kulzer, Wehrheim, Germany) as described by the manufacturer. Briefly, sponge tissue blocks were dehydrated by an ethanol series in 70, 90 and 96% (v/v) ethanol for 1 h each, and a final treatment in 99% ethanol (v/v) for 2 h. The pre-infiltration of the dehydrated samples was performed in an 1:1 mixture of 99% ethanol (v/v) and Technovit 7100 for at least 2 h. For the final infiltration, 1.0 g of Technovit hardener was solved in 100 ml base-liquid 100% Technovit, and the samples were subsequently infiltrated over night. For the embedding of the sponge samples, the infiltrated material was transferred into embedding solution (1 part of Technovit hardener II and 15 parts of infiltration solution). The polymerization of the samples was performed by incubation of the embedded sponge material for 1 h at room temperature, followed by the final incubation for 2 h at 30°C in the dark. All steps were carried out under vacuum using a desiccator equipment. Polymerized sponge tissue blocks were trimmed with a small circular saw. Sections of 20-μm thickness were cut with a steel knife at the rotary microtome.

2.2. Hybridization procedure

For in situ hybridization of sponge sections the following oligonucleotide probes were used: (i) probe EUB338, specific for the domain *Bacteria* (Amann et al., 1990), (ii) probe SRB385Db, specific for most members of delta subclass *Proteobacteria* including *Desulfobacteriaceae* (Rabus et al., 1996), (iii) probe DSV1292, specific for *Desulfovibrio desulfuricans* and relatives (Manz et al., 1998). The Cy3-labeled oligonucleotide non-EUB338, which has the complementary (antisense) sequence to probe EUB338 served as a negative control for nonspecific binding. Custom synthesized oligonucleotides were purchased 5′-labeled with the indocarbocyanine dye Cy3 (CyDye™, Amersham Pharmacia Biotech Europe, Freiburg, Germany) and Oregon Green (Molecular Probes Inc., Eugene, OR) from Biometra (Göttingen, Germany) and Metabion (Ebersberg, Germany), respectively. All oligonucleotides were stored in TE buffer (10 mM Tris, 1 mM EDTA, pH 7.5) at −20°C. Working solutions were adjusted to 50 ng DNA per μl. Pre-warmed hybridization solution (0.9 M NaCl, 20 mM Tris–HCl [pH 7.2], 0.01% SDS, 35% [v/v] formamide) was mixed with fluorescently labeled oligonucleotide (1 ng per μl hybridization solution).

Fixed slices of sponge tissue were hybridized by addition of 30 μl hybridization solution and 3 ng labelled probe applied on spots of 5 mm diameter to each tissue slice and incubated for at least 5 h at 46°C. After this, unbound oligonucleotides were removed by gently rinsing with washing buffer (20 mM Tris–HCl, 0.01% SDS, 88 mM NaCl) and incubated at 48°C for 20 min. Before microscopic analysis, hybridized tissues slices were carefully rinsed with distilled water, air dried and mounted in antifading glycerol medium (Citifluor AF2, Citifluor Ltd., London, UK). All hybridization and washing steps were performed in the dark.

2.3. Widefield deconvolution epifluorescence microscopy (WDEM)

Epifluorescence microscopy was performed with a widefield Zeiss Axioplan microscope (Oberkochen, Germany) equipped with a high-pressure mercury arc lamp (HBO 50, Zeiss) and Zeiss filter sets no. 09 (excitation 450–490 nm, dichroic mirror 510 nm, suppression 520 nm), and no. 15 (excitation 546 nm, dichroic mirror 580 nm, suppression 590 nm), corresponding to the excitation and emission maxima of the fluorochromes Oregon Green and Cy3, respectively. To reduce photobleaching, illumination was controlled by an Uniblitz shutter device D 122 (Vincent Associates, Rochester, NY). A piezo-mover

(Physik Instrumente, Waldbronn, Germany) was attached to a infinity color-corrected 63× Plan-Apochromat, oil immersion objective with a numerical aperture of 1.4 (Zeiss, Oberkochen, Germany). Real color images were acquired using a two-stage Peltier cooled CCD-camera (PCO Computer Optics, Kehlheim, Germany) with a spectral range of 290–1000 nm. The 2/3″ sized CCD chip consists of 1280 (H) × 1024 (V) pixel, each 6.7 × 6.7 μm in size. Due to the RGB mosaic filter the real resolution was lowered by a factor of the square root. The dynamic range was 24 bit (8 bit each colour). When using the 63× objective, the voxel size was 100 × 100 nm × z distance (z = 250 or 500 nm).

2.4. Image data acquisition and processing

The general flow for the data acquisition and image processing is given in Fig. 1. For the acquisition of the image stacks and for their subsequent processing the Metamorph Imaging software (Universal Imaging Corporation, West Chester, PA) in conjunction with the EPR-deconvolution software (Scanalytics, Billerica, MA) were used. Calculations were performed using a 200-MHz personal computer running under Microsoft Windows 95. Image data collection was carried out by sampling of data stacks comprising up to 21 digital images obtained from real color images and stored in TIFF format for

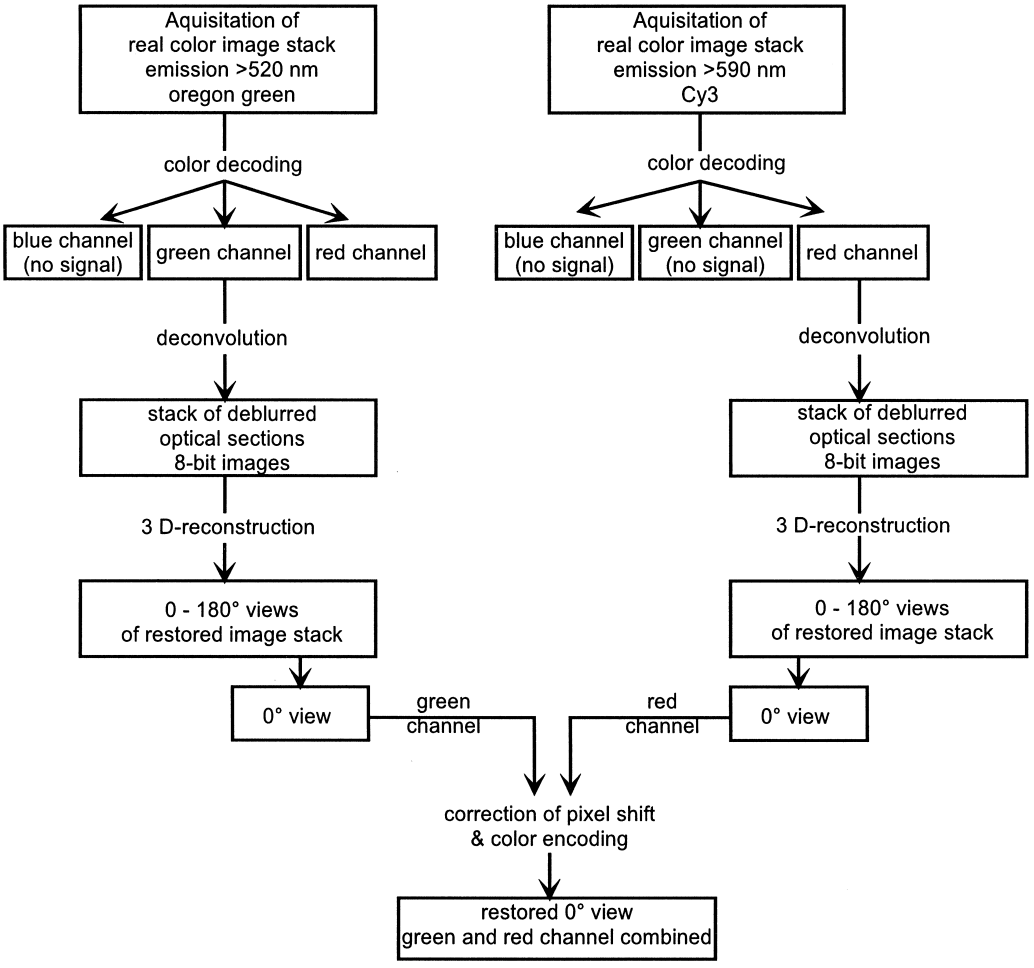

Fig. 1. Flow chart of acquisition and processing of digital image stacks for deconvolution and three-dimensional reconstruction.

subsequent digital image analysis. Spacing along the *z*-axes in increments of 0.25 or 0.5 μm turned out to be suitable in most cases. Consequently, 15–20-μm thick sponge sections could be conveniently processed. Dependent on the samples and fluorochromes used for labelling, the exposure times varied between 800 ms to 1.5 s for each single image. Prior to photon reassignment and three-dimensional image restoration, the acquired real color image stacks were color decoded. For this purpose the red and green channel was processed separately and the image data were combined afterwards to form a deblurred, three-dimensional real color image stack. Usually, the processing of one channel covering the emission maximum was by far sufficient.

The EPR-deconvolution software has to be calibrated by measured point spread functions of fluorescent beads of a size below optical resolution. The fluorescence emission spectra of the beads should be comparable to the fluorescent emission spectra of the sample or fluorophore used. For this purpose, 200 nm-sized Nile red fluorescent polystyrene beads were analyzed (FluoSpheres, Molecular Probes Inc., Eugene, OR) which have broad excitation and emission bandwidths (excitation maximum 535 nm, emission maximum 575 nm) suitable for the used filter sets (Haugland, 1996).

3. Results and discussion

3.1. Sample embedding and sectioning

Embedding of biological specimen in paraffin and plastics prior to sectioning and subsequent FISH is discussed rather controversially in the literature (Poulsen et al., 1994; Licht et al., 1996; Rothemund et al., 1996; Moter et al., 1998). In this study, sections of the paraffin and Technovit embedded sponge tissues were obtained with defined thickness of 15–20 μm and tissue slices were subsequently mounted on silanized glass slides. With regard to autofluorescence of the matrix used for embedding, no specific improvement by using the Technovit could be observed. In contrast to the paraffin sponge tissue blocks, cutting of Technovit sections with the rotary microtom was more difficult and slices could be hardly mounted even on silanized glass slides.

3.2. Deconvolution microscopy of sponge associated bacteria

Fluorescence in situ hybridization (FISH) of paraffin sections of *Chondrosia reniformis* using the *Bacteria* specific probe EUB338 (Oregon Green labeled) and subsequent 3D reconstruction resulted in a strongly blurred image caused by high levels of out-of-focus fluorescence emitted from the sponge tissue. In consequence, the maximum optical resolution which could be obtained by conventional epifluorescence microscopy remained fairly low. This hindered the visualization of details within the sponge sections and the spatial arrangement of the hybridized cell could not be thoroughly resolved (Fig. 2A).

The application of the calibrated deconvolution algorithm after sampling of a stack of 21 optical sections through the identical object shown in Fig. 2A resulted in a remarkable higher optical resolution (Fig. 2B). Specific cell features of sponge associated bacteria could not be shown by classical epifluorescence microscopy (Fig. 2C). In contrast to this, the application of the EPR deconvolution algorithm for stacks of optical sections followed by rendering with the maximum option using the brightest pixels along the line of sight provided detailed information on the cell shape, inclusion bodies and growth states of the corresponding bacteria (Fig. 2D, arrow indicated). Additionally, the spatial arrangement of the sponge associated bacteria within the sponge tissue could be determined. Simultaneous hybridization of *Chondrosia reniformis* with the *Bacteria* specific probe EUB338 (Oregon Green-labeled) and the Cy3-labeled probe SRB385Db resulted in a highly blurred image obtained from the unprocessed optical sections (Fig. 3A. Application of the deconvolution algorithm to the identical optical sections shown in Fig. 3A visualized not only large amounts of small bacterial cells hybridizing with probe EUB338, but also revealed dividing cells hybridizing with probe SRB385Db (Fig. 3B, indicated by arrows).

The photomicrographs given in Fig. 3C and D show the maximum pixel enlargement of an unprocessed extended image projection obtained by widefield epifluorescence microscopy (Fig. 3C) compared with the maximum resolution achieved for the same object after deconvolution rendering of a series

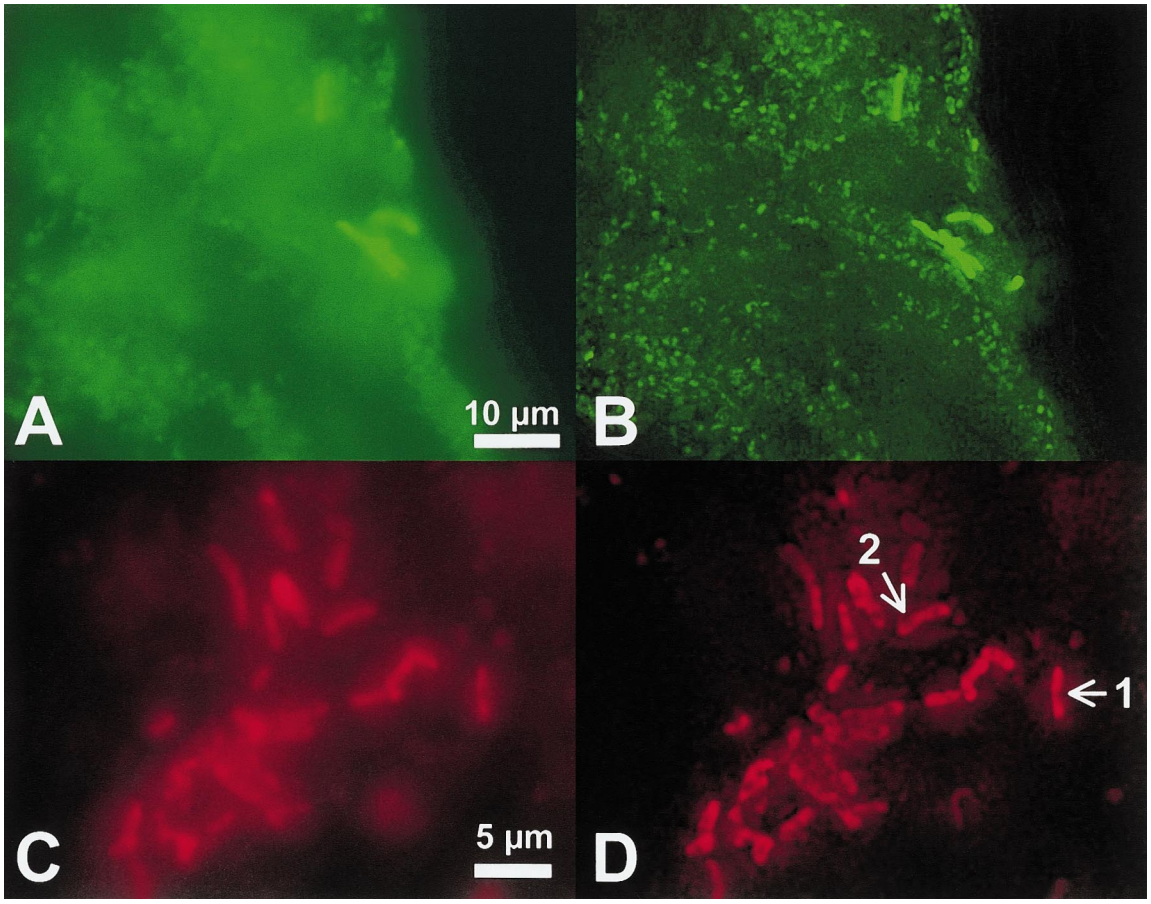

Fig. 2. Comparison of conventional and deconvolution epifluorescence photomicrographs of tissue sections of *Chondrosia reniformis* after hybridization with the *Bacteria* specific probe EUB338 ([A, B] Oregon Green-, [C, D] Cy3-labeled). Twenty one optical sections were obtained along the optical axis with increments of 0.25 μm. (A) Extended focus image obtained by projection of all optical sections without prior removal of out-of-focus signals. Fine structures remain almost invisible within the blurred image. (B) Extended focus image of the identical tissue section shown in (A) after deconvolution processing of the image stack using the EPR algorithm. Note numerous small coccoid *Bacteria* within the sponge mesohyl and rod-shaped bacteria colonizing the channel system of the sponge cortex. (C) Extended focus image obtained by projection of unprocessed image data showing a blurred microcolony of rod shaped bacteria. (D) Identical focus image given in (C) after application of deconvolution algorithm resulting in the visualization of specific cell features such as dividing states (indicated by arrow 1) and inclusion bodies (indicated by arrow 2).

Fig. 3. Comparison of conventional and deconvolution epifluorescence photomicrographs of *Chondrosia reniformis* after FISH with oligonucleotides on different phylogenetic levels. (A) Extended focus image of a series of 21 unprocessed optical sections obtained after hybridization with *Bacteria* specific probe EUB338 (Oregon Green-labeled) and Cy3-labeled probe SRB385Db. (B) Extended focus image obtained by projection of the identical image stack shown in (A) after deconvolution processing resulting in the detailed population analysis and the visualization of specific cell states (dividing cells indicated by arrows). (C and D) Detailed view of images given in (A) and (B) showing the maximum pixel enlargement for conventional epifluorescence (C) and the improved resolution after application of the deconvolution algorithm (D). (E) Extended focus image generated by projection of unprocessed serial sections obtained with the red channel of the CCD camera showing a blurred microcolony of bacteria hybridizing with the Cy3-labeled probe DSV1292. (F) Extended focus image of the identical tissue section shown in (E) after deconvolution processing. The combined color-encoded green and red channel projection shows the *Desulfovibrionaceae* stained with the Cy3-labeled probe DSV1292 surrounded by large amounts of coccoid cells within the sponge mesohyl simultaneously hybridizing with the *Bacteria* specific probe EUB338 (Oregon Green-labeled). All pictures were done at a magnification of $\times 630$.

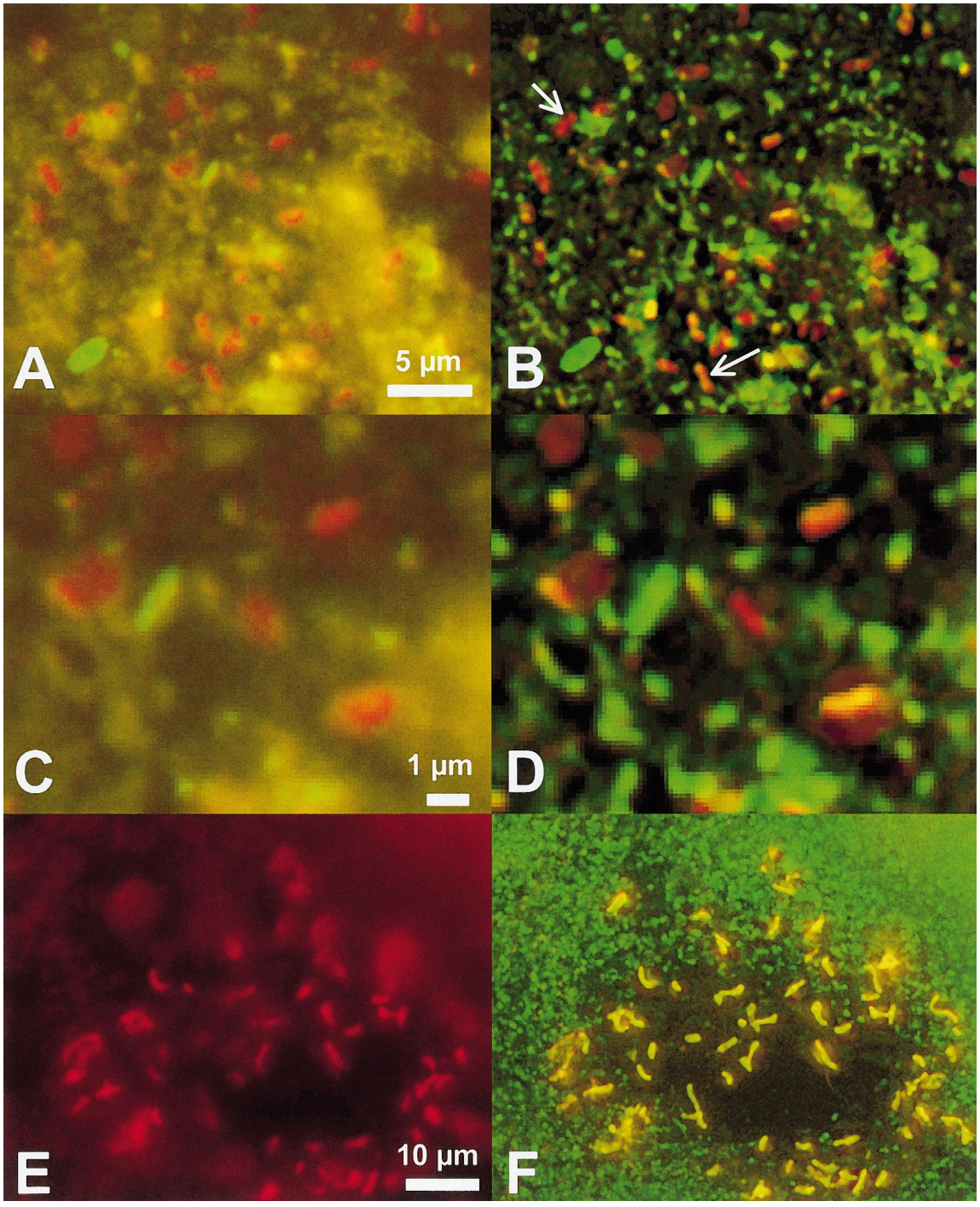
A
5 µm
B
C
1 µm
D
E
10 µm
F

of 21 digital images acquired with increments of 0.25 μm each (Fig. 3D). Whereas the cell boundaries of the bacteria in images obtained by conventional epifluorescence microscopy could not be resolved, application of the deconvolution algorithm to images obtained from the same specimen showed clearly distinguishable cell boundaries and allowed the analysis of dividing cells forming defined microcolonies.

3.3. Visualization of the spatial arrangement of sponge associated bacteria in Chondrosia reniformis

For the first time, great amounts of coccoid cells (average cell diameter 0.7 μm) located within the sponge mesohyl could be successfully visualized (Fig. 2B). Some of the rod shaped cells on the surface of the sponge cortex were remarkably enlarged (4 μm in length, 1 μm in width) and showed significantly stronger fluorescence signal intensities compared to other sponge associated bacteria (Fig. 2B). Detailed analysis of the distribution of the sponge associated cells within different parts of the sponge revealed that microcolonies formed by strongly fluorescent, rod shaped bacteria were always directly located at micropores of *Chondrosia reniformis*. The putatively higher metabolic potential of these cells might be caused by the additional accessibility of electron acceptors (e.g. sulfate from the ambient seawater) and/or the improved availability of substrates through the sponge channel system. The application of a top-to-bottom directed approach using rRNA targeted oligonucleotide probes revealed the phylogenetic affiliation and three-dimensional arrangement of sulfate-reducing bacteria (SRB) among the sponge associated bacterial community. SRB play an important role in pyritization within marine systems as previously discussed (Reitner and Schumann-Kindel, 1997). The presence of culturable SRB originating from sponge material could be recently demonstrated by the application of specific in situ probes (Schumann-Kindel et al., 1997). However, a defined three-dimensional localization of the SRB within the natural structure of the sponge tissue could not be shown yet. In the present study, hybridization of thin sections of paraffin and Technovit embedded sponge material revealed large numbers of cells hybridizing with the *Bacteria* specific probe EUB338, and 20% (± 4.2) of the total cell counts emitted strong fluorescent signals after hybridization with the SRB specific probe SRB385Db (Fig. 3B). Again, the application of deconvolution processing remarkably improved the optical resolution and showed the typical morphology of dividing cells within the SRB population in the sponge mesohyl (Fig. 3B, indicated by arrows).

Further detailed analysis of the sponge associated SRB population performed with probes on more narrow phylogenetic levels elucidated the presence of microcolonies hybridizing with the Cy3-labeled probe DSV1292, indicating members of the family *Desulfovibrionaceae* (Fig. 3E,F). The simultaneous application of Oregon Green-labeled probe EUB338 and Cy3-labeled probe DSV1292 followed by deconvolution processing showed that the microcolony of *Desulfovibrionaceae* within the sponge channel system was densely surrounded by coccoid cells with an average cell diameter of 0.7 μm which formed the vast majority of the sponge associated bacteria within the mesohyl (Fig. 3F). Caused by the overlay of green and red fluorescence, SRB appear yellow in Fig. 3F.

3.4. Key features of widefield deconvolution microscopy

The most critical point during the deconvolution image process is the calibration of the point spread function. Depending on the CCD camera used, a high signal to noise ratio and high optical resolutions can be realized. Since no laser beam is necessary for illumination, photobleaching of fluorochromes or photodamage of the investigated specimen is less critical than using confocal laser scanning microscopy which require laser beams emitting high photon densities. Confocal laser scanning microscopy offers the possibility to directly acquire 2D imaging of 3D objects, but the maximum signal to noise ratio and the optical resolution of confocal laser scanning microscopy is lower than using widefield epifluorescence microscopy coupled with deconvolution rendering.

While mathematical approaches for deblurring microscopic images are less expensive than hardware-based optical sectioning methods, there are

limitations to the number of depths that may be used during the calculation as well as to the complexity of the image. For example, the deconvolution of 10–20 slices per object requires a complex calculation process, and the time for iterative calculations required with the PC system described above up to 8 h of processing. In order to reduce the number of slices necessary for optimum deconvolution efficiency, the combination of thin-sectioning methods and deconvolution processing seems to be appropriate for the analysis of more complex specimen at present. In this study, sampling usually comprised up to 21 slices, originated from series of *z*-steps with 0.25–0.5-μm wide increments.

In the near future, the development and application of further deconvolution algorithms, e.g. blind deconvolution algorithms which do not require the calibration of the point spread function, and the availability of more powerful personal computers may provide easier and faster handling of deconvolution microscopy and will significantly reduce the calculation time needed for more complex images.

Acknowledgements

The authors gratefully acknowledge the support from the Deutsche Forschungsgemeinschaft (Re 665/12-1 LEIBNIZ-Award). This publication is contribution no. 16 of the Collaborative Research Center SFB 468 'Wechselwirkungen an geologischen Grenzflächen' at the University of Göttingen, Teilprojekt A1, also funded by the Deutsche Forschungsgemeinschaft.

References

Amann, R., Krumholz, L., Stahl, D.A., 1990. Fluorescent-oligonucleotide probing of whole cells for determinative, phylogenetic, and environmental studies in microbiology. J. Bacteriol. 172, 762–770.

Amann, R.I., Ludwig, W., Schleifer, K.-H., 1995. Phylogenetic identification and in situ detection of individual microbial cells without cultivation. Microbiol. Rev. 59, 143–169.

Carrington, W.A., Fogarty, K.E., Lifschitz, L., Fay, F.S., 1995. Three-dimensional imaging on confocal and wide-field microscopes. In: Pawley, J.B. (Ed.), Handbook of Biological Confocal Microscopy, Plenum Press, New York, pp. 151–161.

Gerrits, P.O., Smid, L., 1983. A new, less toxic polymerization system for the embedding of soft tissues in glycol-methacrylate and subsequent preparing of serial sections. J. Microsc. 132, 81–85.

Haugland, R.P., 1996. Handbook of Fluorescent Probes and Research Chemicals, Molecular Probes, Eugene, OR.

Holmes, T.J., Bhattacharyya, S., Cooper, J.A., Hanzel, D., Krishnamurthi, V., Lin, W., Roysam, B., Szarowski, D., Turner, J., 1995. Light microscopic images reconstructed by maximum likelihood deconvolution. In: Pawley, J.B. (Ed.), Handbook of Biological Confocal Microscopy, Plenum Press, New York, pp. 389–402.

Lawrence, J.R., Korber, D.R., Wolfaardt, G.M., Caldwell, D.E., 1996. Analytical imaging and microscopy techniques. In: Hurst, C.J., Knudsen, G.R., McInerney, M., Stetzenbach, L.D., Walter, M.V. (Eds.), Manual of Environmental Microbiology, American Society for Microbiology Press, Washington, DC, pp. 29–51.

Licht, T.R., Krogfelt, K.A., Cohen, P.S., Poulsen, L.K., Urbance, J., Molin, S., 1996. Role of lipopolysaccharide in colonization of the mouse intestine by *Salmonella typhimurium* studied by in situ hybridization. Infect. Immun. 64, 3811–3817.

MacNaughton, S.J., Booth, T., Embley, T.M., O'Donnell, A.G., 1996. Physical stabilization and confocal microscopy of bacteria on roots using 16S rRNA targeted fluorescent-labeled oligonucleotide probes. J. Microbiol. Methods 26, 279–285.

Manz, W., Amann, R., Ludwig, W., Wagner, M., Schleifer, K.-H., 1992. Phylogenetic oligodeoxynucleotide probes for the major subclasses of proteobacteria: problems and solutions. System. Appl. Microbiol. 15, 593–600.

Manz, W., Amann, R., Szewzyk, R., Szewzyk, U., Stenström, T.-A., Hutzler, P., Schleifer, K.-H., 1995. In situ identification of *Legionellaceae* using rRNA-targeted oligonucleotide probes and confocal laser scanning microscopy. Microbiology 141, 29–39.

Manz, W., Eisenbrecher, M., Neu, T.R., Szewzyk, U., 1998. Abundance and spatial organization of gram-negative sulfate-reducing bacteria in activated sludge investigated by in situ probing with specific 16S rRNA targeted oligonucleotides. FEMS Microbiol. Ecol. 25, 43–61.

Moter, A., Leist, G., Rudolph, R., Schrank, K., Choi, B.K., Wagner, M., Göbel, U.B., 1998. Fluorescence in situ hybridization shows spatial distribution of yet uncultured treponemes in biopsies from digital dermatitis lesions. Microbiology 144, 2459–2467.

Poulsen, L.K., Lan, F., Kristensen, C.S., Hobolth, P., Molin, S., Krogfelt, K.A., 1994. Spatial distribution of *Escherichia coli* in the mouse large intestine inferred from rRNA in situ hybridization. Infect. Immun. 62, 5191–5194.

Rabus, R., Fukui, M., Wilkes, H., Widdel, F., 1996. Degradative capacities and 16S rRNA-targeted whole cell hybridization of sulfate-reducing bacteria in an anaerobic enrichment culture utilizing alkylbenzenes from crude oil. Appl. Environ. Microbiol. 62, 3605–3613.

Reitner, J., Schumann-Kindel, G., 1997. Pyrite in mineralized sponge tissue. Product of sulfate reducing sponge-related bacteria? Facies 36, 272–276.

Rothemund, C., Amann, R., Klugbauer, S., Manz, W., Bieber, C.,

Schleifer, K.-H., Wilderer, P., 1996. Microflora of 2,4-dichlorophenoxyacetic acid degrading biofilms on gas permeable membranes. Syst. Appl. Microbiol. 19, 608–615.

Schumann-Kindel, G., Bergbauer, M., Manz, W., Szewzyk, U., Reitner, J., 1997. Aerobic and anaerobic microorganisms in modern sponges: A possible relationship to fossilization processes. Facies 36, 268–272.

Shaw, P.J., Rawlins, D.J., 1991. The point-spread function of a confocal microscope: its measurement and use in deconvolution of 3D data. J. Microsc. 163, 151–165.

Wagner, M., Assmus, B., Hartmann, A., Hutzler, P., Amann, R., 1994. In situ analysis of microbial consortia in activated sludge using fluorescently labelled, rRNA-targeted oligonucleotide probes and confocal laser scanning microscopy. J. Microsc. 176, 181–187.